



Effectiveness of Various Techniques Using FRP for the Strengthening of R. C. Beams with Tension Lap Splices

Mohamed H. Makhlof^{1*}

¹*Department of Civil Engineering, Benha Faculty of Engineering, Benha University, Egypt.*

Author's contribution

The sole author designed, analyzed, interpreted and prepared the manuscript.

Article Information

DOI: 10.9734/JERR/2019/v6i116937

Editor(s):

(1) Dr. Tian- Quan Yun, Professor, School of Civil Engineering and Transportation, South China University of Technology, China.

Reviewers:

(1) Jianhui Yang, Henan Polytechnic University, China.

(2) Shashidhar K. Kudari, CVR College of Engineering, India.

Complete Peer review History: <http://www.sdiarticle3.com/review-history/49847>

Original Research Article

Received 10 April 2019

Accepted 21 June 2019

Published 27 June 2019

ABSTRACT

This paper presents an experimental program conducted to investigate the flexural performance of RC beams with tension reinforcement lap splice strengthened using externally bonded FRP different techniques in splice region. The specimens were reinforced on the tension side with four deformed bars spliced at mid span. The tested beams are of 3200 mm total length and 250*120 mm cross section, tested in positive bending. The considered parameters were splice length, type of FRP (glass or carbon), strengthening techniques in splice region (externally confine strips around cross section, Near Surface Mounted technique "NSM" stirrups, externally bonded sheets or bars on the tension face, number of GFRP strips layers (one layer, two layers, and three layers), and shape of NSM stirrups (Box or U shape). No additional anchorage mechanism or bonding methodology was applied for the FRP strips on the concrete except the epoxy adhesive. The effect of these factors on the failure of modes, the ultimate load, the bond strength and that the ductility were investigated. The results indicated that all applied strengthening techniques were efficient in improving the bond strength of the lap splices, the ductility, and the load-deflection behavior of the tested beams, especially when strips were installed over the splice region. This study approved that NSM technique gave more prominent simplicity of employ.

*Corresponding author: Email: mohamedmakhlof83@yahoo.com;

Keywords: Near-surface mounted; ductility; FRP; lap splices; bond strength; techniques.

1. INTRODUCTION

The overall structural performance of R.C. elements is mainly dependent on the bond characteristics between reinforcing steel bars and the surrounding concrete. Therefore, when reinforcing steel bars is spliced in concrete beam, it is needed to overlap the bars adequate long for tensile stresses in one bar to be fully shifted to other bars without inducing a pullout failure in the concrete moreover, the required transverse reinforcement at the spliced zone. Unrelatedly of concrete type, the failure of specimens with lap splices without crosswise reinforcement was violent and happened within the entire length of the splice. Adding suitable confinement along the splice zone improved the behavior as the proper confinement eliminated the creation of splitting cracks at tension splice zone [1,2,3,4,5]. Studying the ductility of reinforced concrete beams with lap splices is very substantial; ductility might be expressed as the ability to under-go deformation without an essential reduction in the capacity of the member [6]. Ductility of the concrete system represents a major role in structural behavior, especially in particular purposes like structures exhibition to earthquake, where ductility plays a vigorous function. For the development of the structural performance of R.C. beams, the FRP from carbon fibers (CFRP) or glass fibers (GFRP) as strengthening material become the excellent choice for its advantages such as high strength, corrosion resisting, light weight and durability [7-17].

Many researchers investigated reinforcement concrete beams flexural strengthened with near-surface-mounted (NSM) technique using FRP bars and strips [18-25]. The application of NSM FRP reinforcement does not needs surface preparation work as in the case of externally bonded FRP reinforcement. Furthermore, the NSM FRP strengthening technique is also very efficient and practical for flexural strengthening of slabs and beams.

In order to overcome the tension lap splice with percentage of lapped steel excess the code limitation at that section and without provision the adequate transverse confinement, the present research introduces externally different techniques to enhance the bond strength of the lap splices and the ductility. The study explores the flexural behavior of R.C. beams strengthened

by various systems mainly by EBR or NSM techniques. Experimental tests have been executed on twelve (12) beams were tested under four point loading till failure, the study parameters were splice length, strengthening techniques, FRP type, number of strips layers, and shape of NSM stirrups.

2. EXPERIMENTAL PROCEDURE

2.1 Specimens and Test Matrix

The construction of the test specimens involved a total of twelve (12) medium-scale simply reinforced concrete rectangular beams of dimensions 120 mm in width, 250 mm in depth, 3200 in length. The specimens were tested under four-point loading as simply supported with an effective span of 3000 mm between the supports and loaded with two equal point loads at middle third of the span. The loading system designed to produce a constant moment region in the middle of the beam. The specimens were reinforced on the tension side with four 12 mm diameter deformed bars spliced at mid span. The splice length of the deformed bars was 550 mm in all beam specimens except third control beam that had 320 mm splice length. The top reinforcement on the compression side consisted of two 10 mm diameter deformed bars. Transverse reinforcement (stirrups) was provided along the beam length, consisted of 8 mm mild steel placed at a spacing of 200 mm. A clear concrete cover of 15 mm was maintained on all sides. Longitudinal and cross section details of the beam specimens are shown in Fig. 1. The details of the beam specimens in each group are shown in Table 1. The first group (One) consists of three beams having different splice length (0, 320, 550 mm) and without strengthening. The second group (Two) consists of four beams were strengthened around spliced region by externally bonded FRP strips, the difference between beams in this group were the FRP wrap-type (glass or carbon) and the number of GFRP layers (one layer, two layers, and three layers). The third group (Three) consists of three beams were strengthened around spliced region by NSM technique, the variables use in third group were the FRP stirrups type (CFRP or GFRP) and the stirrups shape (box shape or U shape). The last group (four) consists of two beams were strengthened at tension side in splice zone with (EBR-Externally Bonded Reinforcement GFRP

sheets or NSM-Near Surface Mounted -GFRP rods).

The control specimen without lap splice was labeled B0. The designation of the other test specimens can be explained as follows. the first two letters indicate the status of the strengthening in the tested specimens (B0 for un-strengthened lap splice zone, BG for strengthened by GFRP, BC for strengthened by CFRP), the numbers in the middle indicates the

length of the lap splice in cm, and the last letter indicates the technique of the strengthening of splice zone in the beam specimen (ST for beams were strengthened around spliced region by externally bonded FRP strips, NS for beams were strengthened around spliced region by NSM -Stirrups, SH for beam was strengthened at tension side in splice zone with Externally Bonded Reinforcement GFRP sheets, NR for beam was strengthened at tension side in splice zone with Near Surface Mounted -GFRP rods).

Table 1. Test matrix

Group	Beam designation	Splice length, L_s (mm)	FRP type	Strengthening systems
One	B0	0	-----	None
	B0-32	320	-----	None
	B0-55	550	-----	None
Two	BG-55-ST1	550	Glass	EBR-transverse Strips around X-sec., one layer
	BG-55-ST2	550	Glass	EBR-transverse Strips around X-sec., two layers
	BG-55-ST3	550	Glass	EBR-transverse Strips around X-sec., three layer
	BC-55-ST2	550	Carbon	EBR-transverse Strips around X-sec., two layers
Three	BG1-55-NS	550	Glass	NSM-transverse Stirrups around X-sec., box-shape
	BG2-55-NS	550	Glass	NSM-transverse Stirrups around X-sec., U- shape
	BC-55-NS	550	Carbon	NSM-transverse Stirrups around X-sec., box-shape
Four	BG1-55-SH	550	Glass	EBR-longitudinal Sheets, U- shape, two layers
	BG2-55-NR	550	Glass	NSM- longitudinal rods, two bars

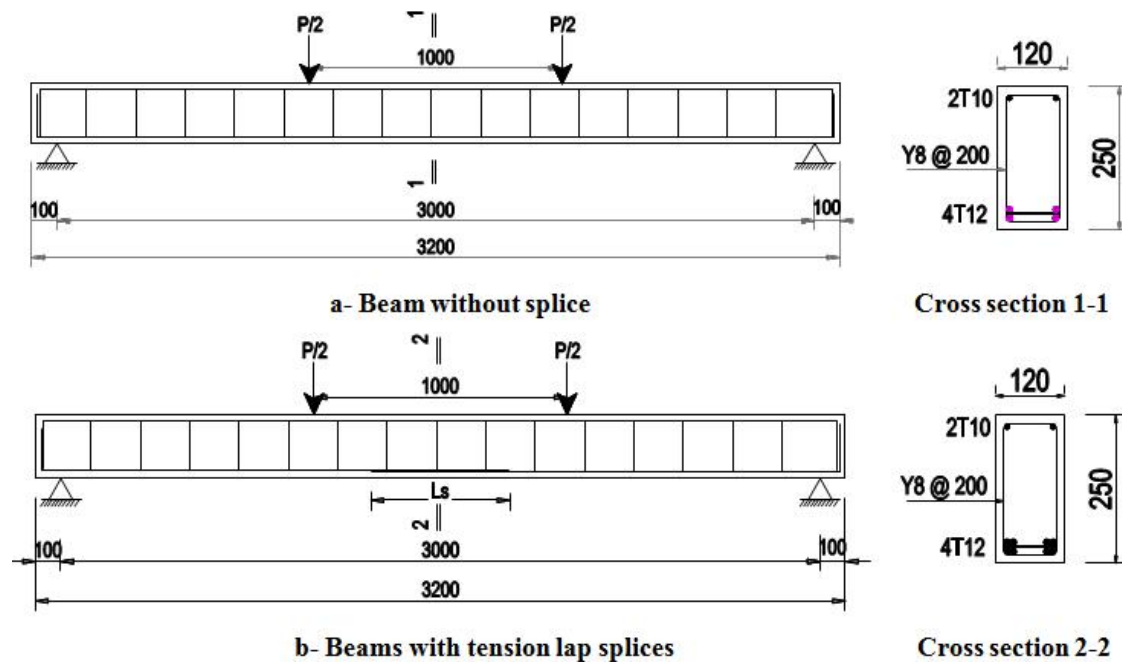


Fig. 1. Longitudinal and cross section details of beam specimens
(Note: all dimensions in mm)

2.2 Materials Properties

2.2.1 Concrete

The materials used in concrete mixture were ordinary Portland cement (OPC- 42.5 grade), natural sand with 2.65 fineness modulus and crushed dolomite with maximum aggregate size 16 mm. The mix design was carried out for 28-day concrete compressive strength (f_{cu}) = 30 MPa. The mix design proportional of cement, fine aggregate and coarse aggregate were (1:1.75:3.50). The water cement ratio by weight was 0.45. Three cubes, 150×150×150 mm, were cast at the same time as the specimens and cured alongside the specimens.

2.2.2 Steel bars

The longitudinal steel were deformed steel with nominal yield strength of 400 MPa used for all beams as top reinforcement and main tension reinforcement, 8 mm diameter of normal mild steel was used for all beams as stirrups with nominal yield strength of 240 MPa. The modulus of elasticity for all steel bars was 200 GPa.

2.2.3 FRP sheets

Unidirectional CFRP and GFRP were used for strengthening the lap splice region. Table 2 illustrated the mechanical properties of the FRP. The FRP were bonded to the beam specimens with an epoxy resin, Sikdature 330. For applying FRP to strengthening the lap splice zone in beam specimens, the bonded faces were cleaned until any loose material was removed. Epoxy adhesive was applied to the concrete face in thin

layer and pre-cut FRP layer was wrapped over it. The sheet in tension face or strips around cross section were passed firmly and rolled uniformly by plastic rollers to squeeze out excess epoxy and air bubbles. For applying more layers, epoxy was poured over the last layer and the procedure was repeated.

2.2.4 GFRP rods

GFRP rods were locally fabricated using pultruded polymer composite; the GFRP rod was manufactured using FRP strip. Initially, the required width of the FRP sheet was calculated based on the same width of used sheet in bottom face of beam. A strip with the design width and required length was cut from an GFRP sheet, then wrapped and placed in the Wooden model on which the straight-shaped grooved was to be manufactured. The mixed of two component epoxy resin was then put on the GFRP .After that, the trapped air was expelled and then surfaces were coated by sand layer to improve its bond. After it is finished, it is left to dry and then remove it from the wooden model and manufacture other. The mechanical properties of GFRP rods were obtained by testing specimen. Table 2 shows the mechanical properties of the FRP bars used in this study.

2.3 Test Setup and Instrumentation

The beams were tested subjected to four- point bending until failure; details of test set-up are shown in Fig. 2. The load was applied through a hydraulic jack and was transferred to the test beam through a steel spreader beam that was

Table 2. Dimensional and mechanical properties of FRP

a) FRP bars		
property		GFRP
Diameter of bars (mm)		8
Area of bars (mm ²)		50
Area of fibers (mm ²)		18.7
Fiber ratio by area		37%
Tensile strength (N/mm ²)		1375
Elasticity modulus (N/mm ²)		66000
Strain at failure		2.10%
b) FRP sheets		
Property	CFRP	GFRP
Fabric design thickness (mm)	0.131	0.170
Strips fabric width (mm)	50	50
Sheets fabric width (mm)	-----	200
Tensile strength (N/mm ²)	4300	2250
Elasticity modulus (N/mm ²)	230000	76000
Strain at failure	1.80%	2.80%

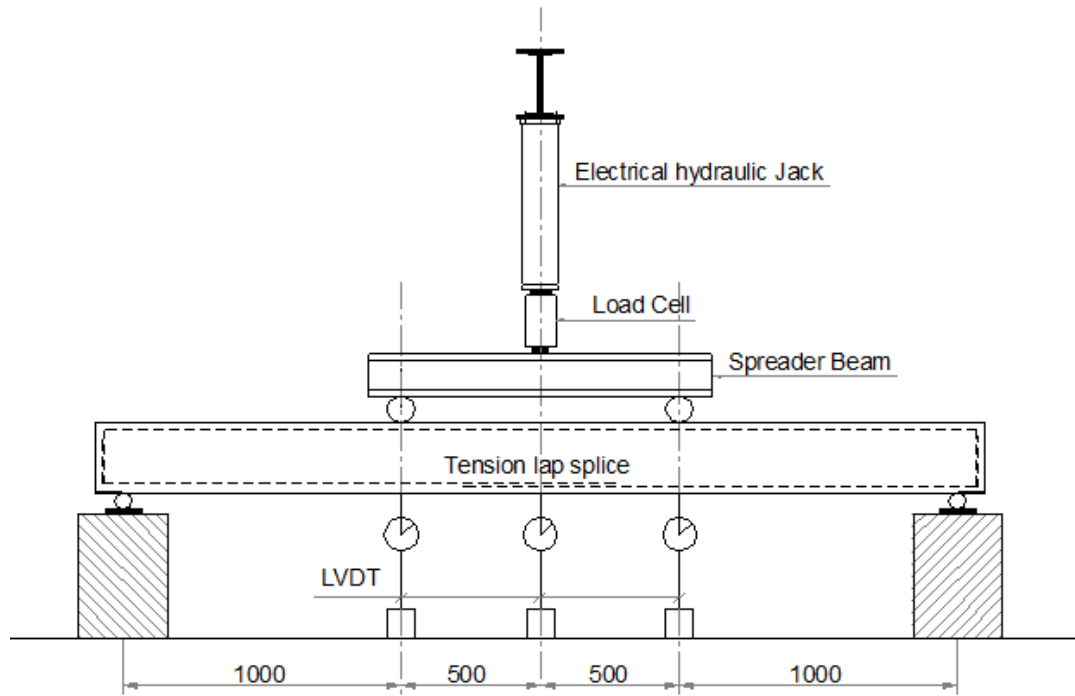


Fig. 2. Schematic view of the test set-up
(Note: All dimensions in mm)

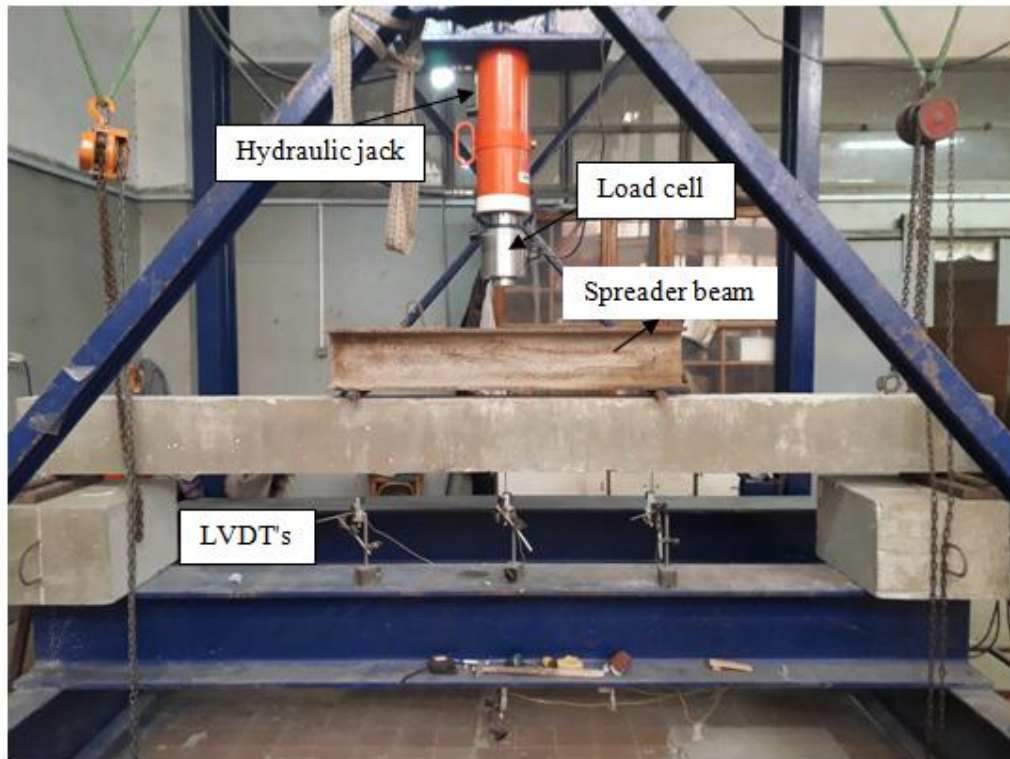


Fig. 3. Specimen beam prior to the test

supported on two steel rollers covering the entire width of the beam. The load was measured using load cell under the hydraulic jack of maximum capacity 1000 kN. Each beam was installed with three linear variable differential transducers (LVDT) placed at the mid-span and directly under the loading point to monitor the deflection Fig. 3 show the photograph of the test setup. The development and propagation of cracks were marked and the mode of failure was recorded.

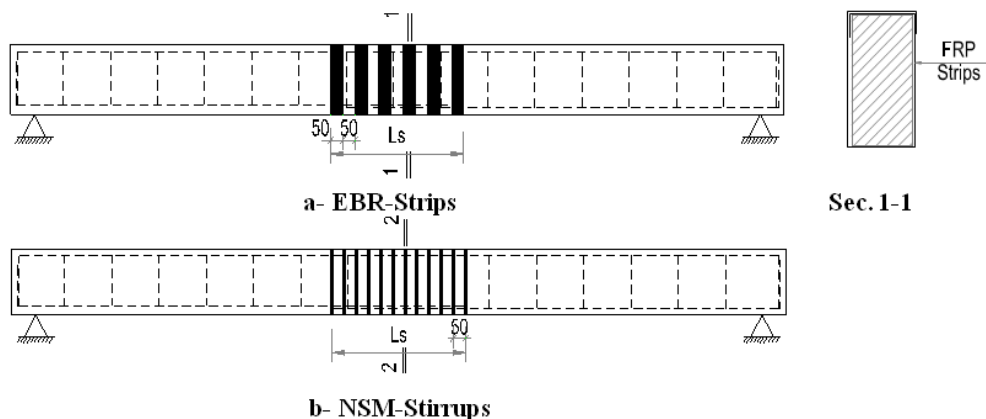
2.4 Fiber-reinforced Polymer Strengthening Systems

2.4.1 Installation of externally bonded FRP (strips or sheets)

In order to achieve a good, strong bond, the surface of the concrete beams was prepared by grinding until the coarse aggregates were exposed and the sharp corners were rounded off, then cleaned by washing and air brushing to remove dust and fine particles. Following cleaning, a uniform thin layer of the epoxy adhesive was applied by palette knife to the surface of the concrete beam. The FRP (strips or sheet) were placed in position on the concrete surface and pressed by hand. To ensure a good bond with concrete, a uniform pressure was applied along the entire length of the (strips or sheets). The FRP strips with 50 mm width and spacing in between equal to the same width of the strip was placed around the cross section of the concrete beams externally bonded FRP transversal reinforcements. As for the externally bonded GFRP sheets U-shaped were placed at the bottom surface with a distance of lap on both sides of the concrete beam 40 mm from each side of the beam as flexural reinforcements (Fig. 4a, 4c).

2.4.2 Installation of NSM FRP (bars or stirrups)

The grooves cut at the surface of the concrete beams had different cross sections depending on the type of strengthening used as shown in Fig. 4b, 4d; the all grooves were approximately 10 mm wide and 10 mm deep. Installation of the NSM FRP reinforcing bars in the longitudinal direction at the tension side of the beam and NSM FRP stirrups around the beam cross section (Box or U-shape) begins by making a series of grooves with specified dimensions cut into the concrete cover of the beam specimens. A special concrete saw with a diamond blade was used to cut the grooves positions shown in Fig. 5. The grooves were cleaned from any dust and air-brushing pressure was used to remove debris and fine particles to ensure proper bonding between the epoxy adhesive and the concrete. The adhesive was applied into the groove before inserting the FRP reinforcing bars or stirrups. Each groove was filled completely with the epoxy adhesive paste using a manual gun to provide the bond with the surrounding concrete. Then the FRP reinforcements (reinforcing bars and transversal stirrups) were inserted inside the grooves ensuring that they were completely covered with epoxy and lightly pressed to displace the bonding agent, this action pressure the epoxy paste to flow around the FRP reinforcement and completely fill the space between the FRP and the sides of the groove. The grooves were then filled with more paste if needed and the excess adhesive was removed, the surface was leveled and smooth finished. The same procedures in terms of cutting the groove, injecting the epoxy, and placing the FRP were applied in two systems of NSM (longitudinal bars or stirrups transversal). The epoxy adhesive was allowed to fully cure at least one week before testing of the beams.



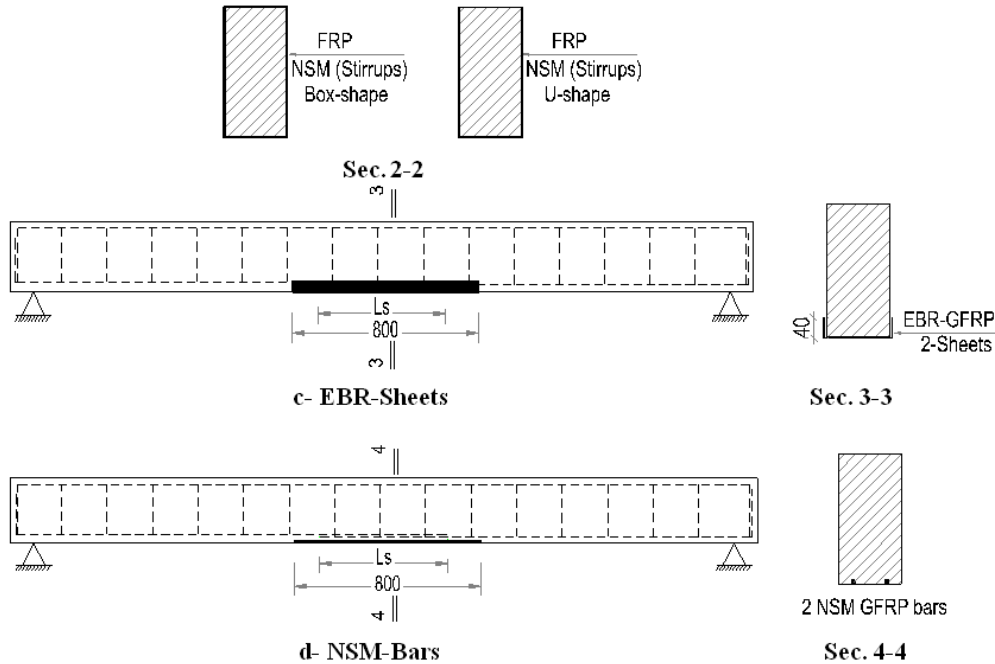


Fig. 4. Description of different FRP techniques
(Note: all dimensions in mm)

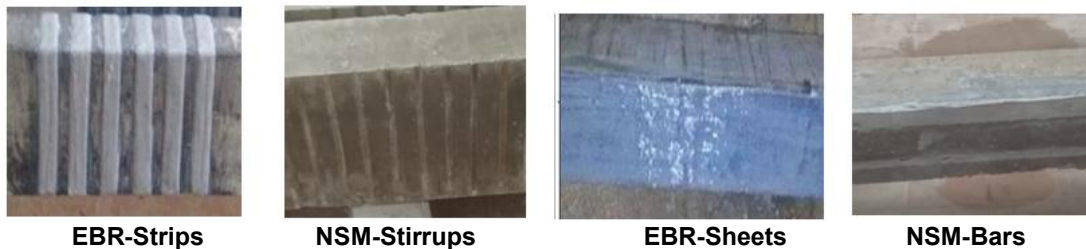


Fig. 5. Strengthening preparation

3. EXPERIMENTAL RESULTS AND DISCUSSION

For the all tested specimens, the relationship between the central deflection at mid-point and the applied load was plotted and the crack propagation was monitored with load increasing till failure. Also, the cracking load and ultimate load were recorded. A brief summary of the test results describing the flexural behavior of all tested beams is presented in Table 3. The results of the B0 without tension reinforcement splice are compared with those of beam specimens with lap splice. Beam B0-55 was tested un-strengthened with tension lap splice and used as a control specimen for comparison purposes to evaluate the improvement in flexural behavior provided by the various NSM and

externally bonded FRP reinforcements. Analysis and discussion of the results are introduced in the following sections.

3.1 Cracking Behavior and Mode of Failure

All the tested specimens were loaded until failed due to flexure. For all specimens, the first crack was recorded, cracks propagation was monitored, and plane of failure was observed to investigate the cracking and failure behavior. Flexural cracks were initiated in all the studied beams occurred randomly in the constant moment region on the tension side of the beam outside the splice length; as the load increased, cracks formed along the entire length of the constant moment region, including the splice

Table 3. Summary of test results

Beam code	P_{cr} (kN)	P_u (kN)	Δ_y (mm)	Δ_u (mm)	Δ_{max} (mm)	Ductility factor μ	Steel stress f_s MPa	Bond stress u_t MPa	Bond ratio	Mode of failure
B0	30	76	21	27	42	2.00	413	NA	NA	Flexure
B0-55	24	67	21	24	30	1.42	365	1.99	1.00	Splitting
B0-32	22	52	19	20	23	1.21	283	1.544	0.78	Splitting
BG-55-ST1	28	75	20	27	40	2.00	409.4	2.233	1.12	Debonding of externally bonded GFRP strips
BG-55-ST2	30	79	20	26	43	2.15	431.2	2.352	1.18	Flexure
BG-55-ST3	30	81	20	25	44	2.20	442.2	2.412	1.21	Flexure
BC-55-ST2	30	80	20	24.3	44	2.20	436.7	2.382	1.20	Flexure
BG1-55-NS	30	72	22	32	42	1.91	393.1	2.144	1.08	Flexure
BG2-55-NS	26	67.3	23	35	40	1.73	367.4	2.004	1.01	Debonding of NSM GFRP U-stirrups
BC-55-NS	31	73.5	22	30	44	2.00	401.2	2.188	1.10	Flexure
BG1-55-SH	25	70	20	22	32	1.60	382.1	2.084	1.05	Debonding of externally bonded GFRP sheet at tension side
BG2-55-NR	24	68	20	23	31	1.55	371.2	2.025	1.02	Splitting

Where, $u_t = f_s d_p / 4l_s$, P_{cr} : 1st. crack load, P_u : Ultimate load, Δ_y : Deflection at yield load, Δ_u : Deflection at P_u , Δ_{max} Deflection at 80% P_u

region. The failure modes of the tested specimens were either a splitting bond failure or ductile flexural failure according to the externally strengthening by the FRP various technique. B0 beam specimen without spliced bars failed in flexure with diagonal compression and tension cracks increasing in ultimate load to fracture in the middle span between two points of loading as shown in Fig. 6a. The beam specimens with spliced bars without a FRP strengthening along the splice length failed suddenly after the initiation of the splitting cracks without any warning or propagation of the cracks accompanied by the loss of the concrete cover over the entire lap splice length, this mode of failure was explosive with high sound which took place in beam B0-32 with splice length of 320 mm, ($26d_b$), under the values recommended by codes, also beam strengthened at tension face by NSM -GFRP rods as shown in Fig. 6b. The strengthening beams with one layer FRP strips, and U-shaped stirrups confining the splice region or with U-shaped sheets at tension face exhibited a gradual failure although the final mode of failure was a face-and-side split failure. Longitudinal splitting cracks started to form in the bottom concrete cover on the tension side directly below the splice region and on the side cover along and adjacent to the lap splices at approximately 90% of the maximum load. The load dropped slightly after reaching a peak when the longitudinal splitting cracks extended across the FRP strips in the splice region. The load continued to gradually drop with increasing deflection. The additional deflections that were imposed to increase the severity of the splitting were halted when failure of the FRP sheets took place. Failure of the FRP sheets or strips was primarily by partial premature debonding or separation of the sheet at the end of the FRP due to high interface shear stresses at this location. Fig. 6c shows the typical debonding failure of the strengthened beams. The flexure cracks of beam specimens strengthening with two layers, three layers of FRP strips, and NSM stirrups extended upward and were very close to the top surface of the beam; very narrow

longitudinal splitting cracks occurred along the splices, without splitting failure. The ductile flexure failure took place by crushing of the concrete in compression nearly the concentrated load. Fig. 6d shows the typical flexure failure of the strengthened beams. Mode of failure for the tested beams is summarized in Table 3.

All strengthening techniques used in this study except the beam strengthened at tension face by NSM -GFRP rods, changed the failure from a splitting sudden failure to a ductile flexural failure.

3.2 Load – Deflection Behavior

The load-deflection behavior of beam with different patterns of FRP systems in the splice region is compared with that of control beam without FRP (B0-55). All the strengthened beams in this study showed an enhancement in the strength and the rigidity compared with the reference beam B0-55. At the same loading level, the deflection values for strengthened beams were lower than that recorded for the reference beam (B0-55), as shown in Figs. 7 to 14.

3.2.1 Effect of splice length

Fig. 7 shows the load-deflection curves of group one; the beams with different lap splice length (0, 320, and 550) mm, the beam B0 without splice showed higher stiffness and ductility. As shown in Fig. 7 it shows decreasing in the ultimate load and increasing in the deflection at the same load for the beams had lap splice in tension zone compared with the reference beam without splice. Reducing the lap splice length from 550 mm to 320 mm led to decrease the ultimate load by 22.3%, also ultimate deflection decrease by 16.6%.

3.2.2 Effect of number of GFRP strips layers

The used number of GFRP strips layers around cross section in splice zone 1, 2, and 3 layers, respectively. The effect of this parameter



Fig. 6a. Flexural failure for B0 beam specimen without spliced

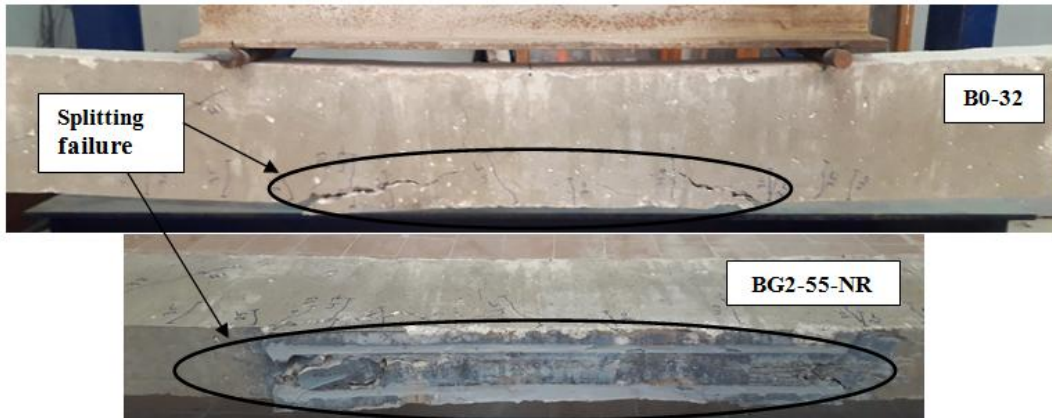


Fig. 6b. Typical splitting (sudden) failure



Fig. 6c. Typical de-bonding/flexural failure



Fig. 6d. Typical ductile flexural failure for strengthened beams

could be observed by studying the behavior of specimens BG-55-ST1, BG-55-ST2, and BG-55-ST3, as shown in Fig. 8. Adding the strengthening layers led to improve the flexural behavior. The ultimate load was higher than that

of control specimen by 11.9%, 17.9% and 20.8% for strengthening number of GFRP layers 1, 2, and 3, respectively. Also, the deflection was reduced by 15%, 25% and 27%, respectively at ultimate recorded load of control specimen.

Comparing the results of lap splice strengthened with different amount of GFRP strips, it can be seen that increasing the number of layers increased the strength of beam specimens. But the maximum load increased slightly when three layers of GFRP strips were placed as compared to one or two layers.

3.2.3 Effect of strengthening materials

The effect of this parameter could be observed by studying the behavior of specimens BG-55-ST2 and BC-55-ST2 for EBR strips technique, also BG1-55-NS and BC-55-NS for NSM stirrups

technique as shown in Figs. 9-10, which correspond to two types of strengthening materials GFRP and CFRP. The both materials used in strengthening led to improve the flexural behavior, where the ultimate load was increased and the deflection at the same loading level was decreased. CFRP were the best material; the ultimate load was increased by 19.4% and 9.7% for specimens strengthened by CFRP strips and NSM CFRP, respectively. However, GFRP strips and NSM GFRP have ultimate load of 117.9% and 107.5%, respectively of the corresponding control beam value. The deflection at ultimate load of B0-55 (control beam) was reduced by

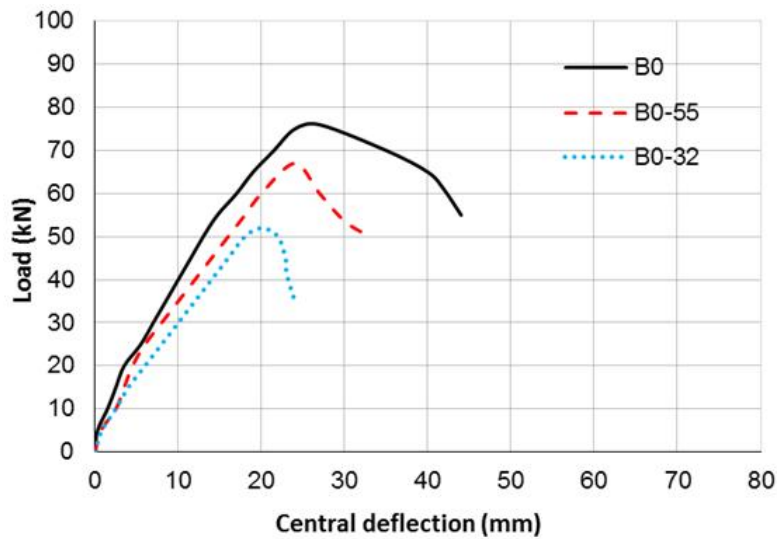


Fig. 7. Effect of splice length on load-deflection relationship (group one)

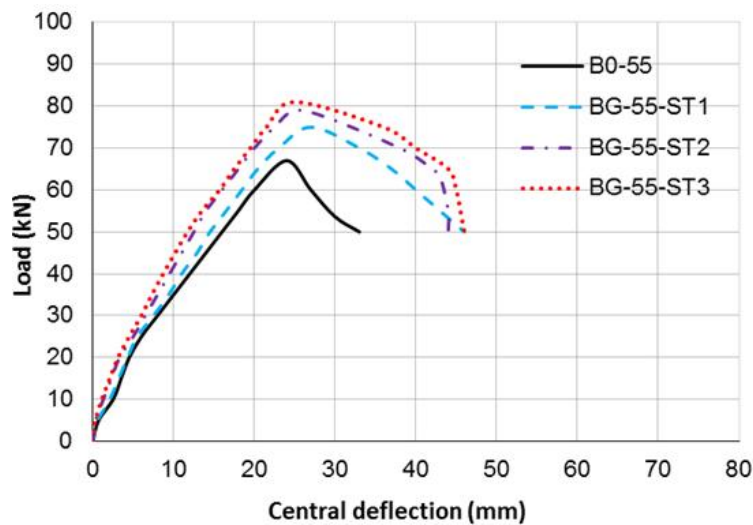


Fig. 8. Effect of number of GFRP strips layers on load-deflection relationships

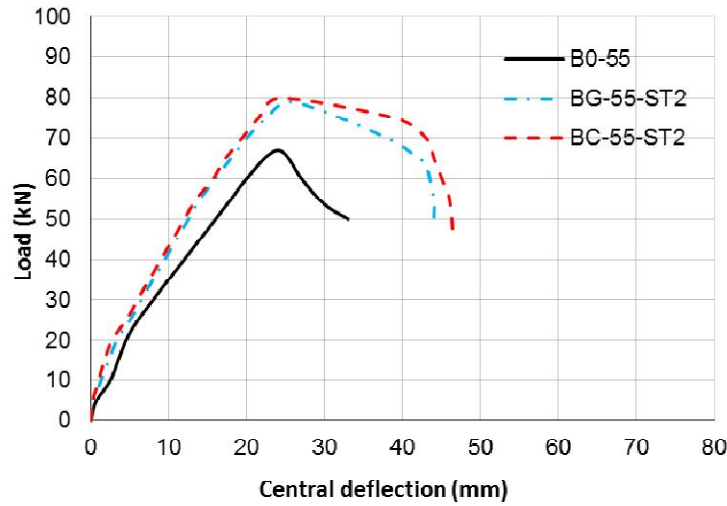


Fig. 9. Effect of the EBR strips fiber type on load-deflection relationships

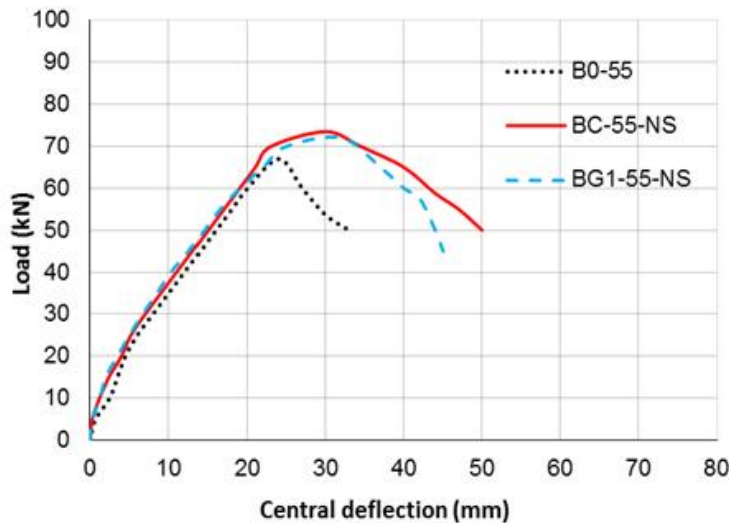


Fig. 10. Effect of the NSM stirrups fiber type on load-deflection relationships

27.9% and 12.5% for specimens strengthened by CFRP strips and NSM CFRP, respectively, also reduced by 25% and 8.3% for specimens strengthened by GFRP strips and NSM GFRP, respectively.

3.2.4 Effectiveness of NSM transverse reinforcement technique and effect of NSM FRP stirrups shape

The load-mid span deflection behavior of strengthened beams with NSM FRP transverse stirrups in comparison with unstrengthened control beam (B0-55) is shown in Fig. 11. This behavior indicates that using NSM FRP

transverse stirrups led to improve the flexural behavior and strength compared with the unstrengthened beam. Using CFRP and GFRP box shape stirrups, an increased in the ultimate strength of 9.7% and 7.5% were measured for beams BC-55-NS and BG1-55-NS, the corresponding increases in the ultimate mid span deflection were 25% and 33.3%, respectively.

Two shape of GFRP NSM stirrups were used in this study, the effect of this parameter could observed by studying the behavior of two beam specimens BG1-55-NS and BG2-55-NS which correspond to two shape of NSM stirrups: box and U shapes, respectively. Changing the shape

from complete stirrups confinement the cross section to U-shape with keeping the same stirrups cross section area led to decrease the ultimate load by 6.5%, not only the ultimate load but also the ultimate deflection increased by 9.4%. These results indicate that the best results obtained when complete stirrups the confinement provided for the lap splice. Also, using the NSM FRP transverse stirrups caused improved the load-deflection behavior and ductility.

3.2.5 Effect of strengthening technique

In this study, four strengthening systems were used; the first two systems were transverse reinforcement technique: bonded FRP strips and NSM stirrups technique, the effect of this parameter could be observed by studying the behavior of two specimens (BG-55-ST1 and BG1-55-NS), respectively as shown in Fig. 12. The second two strengthening systems used in this study as longitudinal reinforcement technique at tension side (bottom face of beams) in splice zone with (EBR- GFRP sheets or NSM-GFRP rods), the effect of this parameter could be observed by studying the behavior of two beam specimens (BG1-55-SH and BG1-55-NR), respectively as shown in Fig. 13.

Using transverse reinforcement technique led to a significant increase in the strength of the strengthened beams in comparison with the control specimen, whether, it is by used EBR GFRP strips or NSM GFRP stirrups. Also, at the

same loading level, lower deflection values were recorded for strengthened specimens, either with EBR GFRP strips or NSM GFRP stirrups, in comparison with the control specimens without strengthened.

On the other side, when used the longitudinal reinforcement technique at tension face of beams in splice zone with EBR- GFRP sheets or NSM- GFRP rods, the ultimate load increased slightly by 4.4% and 1.5% in compared with control beam. The slight improvement is shown in Fig. 13, where the load-deflection responses of beams B0-55, BG1-55-SH and BG1-55-NR are compared.

These results indicate that strengthening techniques effective when confining the tension splice region, whether, it is by used EBR GFRP strips or NSM GFRP stirrups. Another indication the longitudinal reinforcement technique at tension face of beams showed a smaller increase in strength due to early debonding of FRP at failure.

3.3 Cracking and Ultimate Loads

Table 3 presents the first cracking load and ultimate load values for all specimens. The specimen BG-55-ST3 had the highest ultimate load, higher than that control beam by about 21%. This was expected because of the former specimen had the biggest layers of GFRP strips,

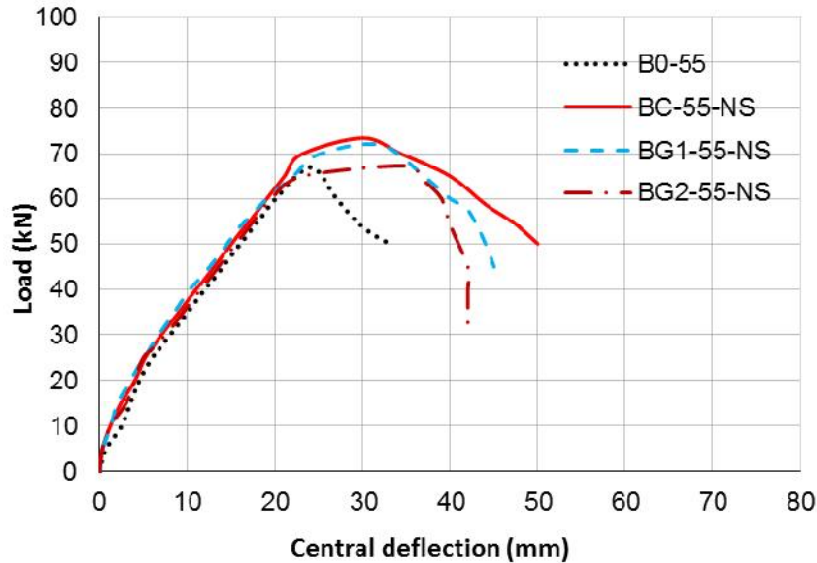


Fig. 11. Effect of the NSM stirrups technique on load-deflection relationships

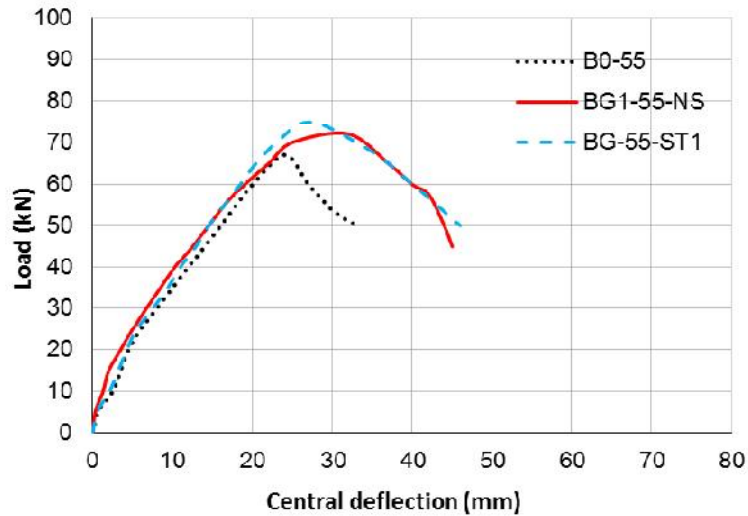


Fig. 12. Effect of the transverse reinforcement technique on load-deflection relationships

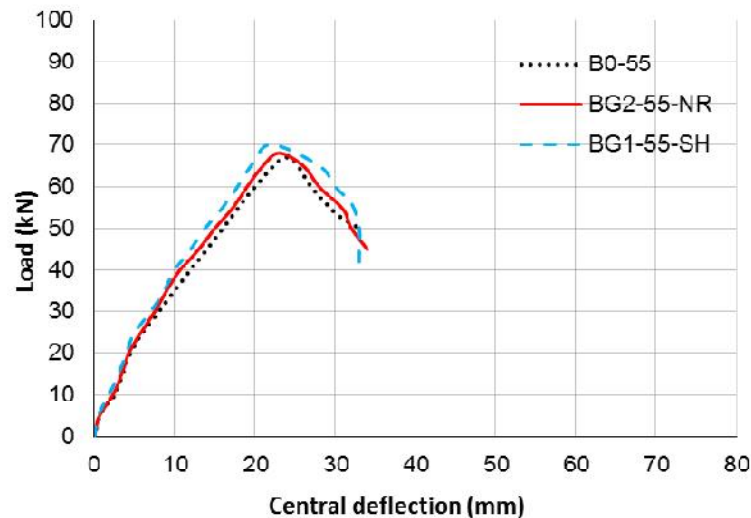


Fig. 13. Effect of the longitudinal reinforcement technique on load-deflection relationships

but the maximum load increased slightly by 2.5% and 8% compared to two layers and one layer, respectively. Fig. 14 shows the comparison of cracking and ultimate loads for all tested specimens. In this study, the effect of used EBR FRP and NSM FRP deleted the impact of splice on cracking load and ultimate load, where the ultimate load of strengthened beams was approximately higher than ultimate load of beam B0 without splice.

3.4 Displacement Ductility

Ductility is the ability of the beam to inelastic deformations beyond the yield deformation

without any considerable loss of load capacity. The displacement ductility ratio (μ), is defined as the ratio between the maximum deflection (the mid span deflection when the load decreased to 80% of the ultimate value along the descending part of the load deflection curve) and the deflection at the point of yielding. As shown in Fig. 15, were indicated by the comparison of the test results of the beam specimens with different strengthening systems, the displacement ductility increased as the result of strengthened, and this increase was more effectiveness with the presence of externally transverse strengthened technique in the splice region, especially when strips were applied over the splice region.

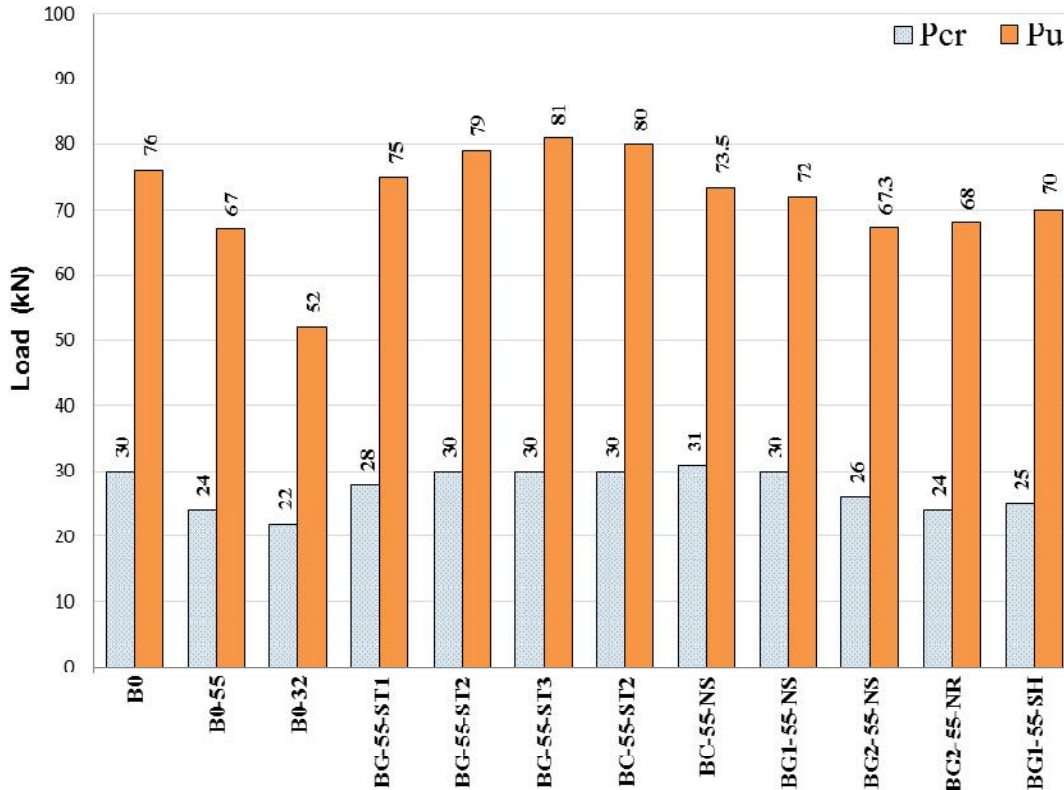


Fig. 14. Cracking and ultimate loads for all beams

As shown in Fig. 15 it shows decreasing in the ductility ratio for the beam which had lap splice in tension zone compared with the (B0) beam without splice by 30%, also, when reducing the lap splice length from 550 mm to 320 mm led to decrease the ductility ratio by 40% in compared to B0. The greatest increase in the displacement ductility was when applied the CFRP strips as strengthening technique around the spliced zone.

Used of the longitudinal reinforcement technique at tension face of beams showed a very slight increase in the ductility due to early debonding of FRP at failure, and that increase did not reach to the ductility of B0 (beam without splice).

Generally, the ductility of specimens strengthened by adding EBR-FRP strips with different numbers of layers around splice region are better than specimens strengthened by NSM-FRP, as shown in Fig. 15, the effect of used EBR-FRP deleted the effect of tension lap splice on ductility, which where the ductility ratio of strengthened beams by FRP strips was higher than ductility ratio of beam B0 without splice.

3.5 Bond Strength

The mode of failure in the beams with tension lap splice was a split failure; this indicated that the splice reached to the maximum capacity. The average bond stress corresponding to the maximum steel stress and the bond ratio are listed in table 3. The stress in the spliced bars f_s was calculated according to ACI 318. To evaluate the average bond stress u_t , the equation (1) was used. The bond ratio is the ratio of bond strength of beam with strengthened divided by the bond strength of a beam B0-55 without strengthened. It is noticed that there was a consistent increase in average bond strength as the result to use the transverse reinforcement techniques, either bonded FRP strips or NSM stirrups technique. When two or three layers of FRP strips were used, the maximum increase in bond strength as compared with the beam without strengthening (B0-55). Both types of FRP had almost the same effect in confining the tension lap splices in beams.

$$u_t = (A_s f_s) / (\pi d_b l_s) = (f_s d_b) / (4 l_s) \quad (1)$$

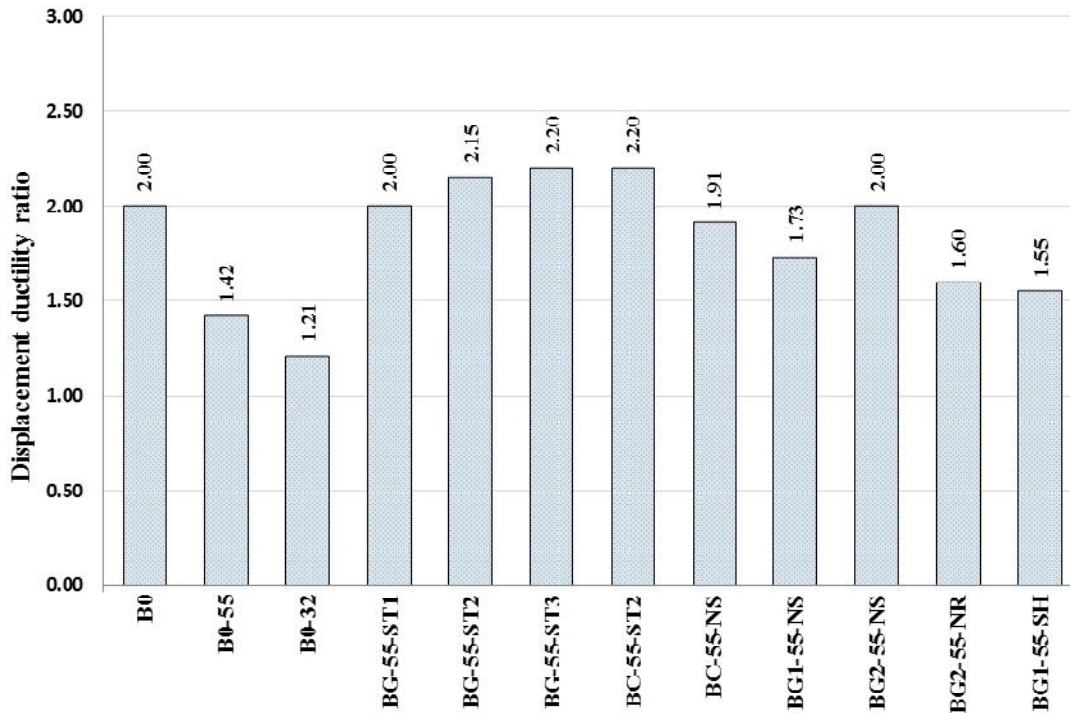


Fig. 15. Displacement ductility ratio comparison for all tested composite beams

4. CONCLUSIONS

Based on the analysis and comparisons of the ultimate load, deflections, mode of failure, ductility ratio, and bond strength of twelve beam specimens designed with different strengthening techniques in splice region, the conclusions obtained in this study were as follows.

1. In the beams with 100% main steel lap splice without strengthened in the splice region, failure occurred after longitudinal splitting, and failure was brittle, sudden, and noisy. The use of NSM GFRP longitudinal bars strengthening technique at tension side did not affect the mode of failure.
2. Transverse strengthening techniques, either bonded FRP strips or NSM stirrups technique were effective in confining the tension splice region, the mode of failure more gradual and more ductile. The final mode of failure changed to a ductile flexural failure.
3. In this study, the effect of used EBR-FRP and NSM-FRP deleted the effect of tension lap splice on cracking and ultimate load, where the ultimate load of strengthened beams was higher than the ultimate load of control beam without splice.
4. Transverse strengthening techniques had positive effect on the deflection behavior, ductility, and increasing the average splitting bond strength, the increase relative to the control beam B0-55 ranged from 8% to 21%.
5. The strengthened beams with (NSM) technique provided a significant increase of ductility and capacity in compared with control beam.
6. The box shape of NSM-GFRP stirrups gave the highest increase in ultimate load, ductility, and bond strength in compared with U-shape. This is mainly due to the increase in bonding.
7. Increasing the number of GFRP layers around splice region leads to increase the stiffness and ductility of beam and therefore, increasing in ultimate load capacity.
8. This study approved that NSM-stirrups technique gave more prominent simplicity of use, give flat surface, and low cost, as well as efficient method for enhancing the stiffness, ductility and flexural strength.

COMPETING INTERESTS

Author has declared that no competing interests exist.

REFERENCES

1. Hamad B, Ali A, Harajli M. Effect of fiber-reinforced polymer confinement on bond strength of reinforcement in beam anchorage specimens. *Journal of Composites for Construction*. 2005;9(1): 44-51.
2. Garcia R, Helal Y, Pilakoutas K, Guadagnini M. Bond behaviour of substandard splices in RC beams externally confined with CFRP. *Construction and Building Materials*. 2014;50:340–351.
3. Magda I. Mousa. Flexural behaviour and ductility of High Strength Concrete (HSC) beams with tension lap splice. *Alexandria Engineering Journal*. 2015;54(3).
4. Mabrouk R, Mounir A. Behavior of RC beams with tension lap splices confined with transverse reinforcement using different types of concrete under pure bending. *Alexandria Engineering Journal*; 2017.
5. Tarek Fawzy, Abdel-Hakim Khalil, Ahmed Atta, Hamdy Afefy, Mohamed Ellithy. Enhancement of tension lap splice in HPC using different techniques. *International Conference on Advances in Structural and Geotechnical Engineering*; 2019.
6. Gamal I. K. Khaleel. Ductility of reinforced concrete beams with lap splices. *CERM*. 1999;21(3):672-691.
7. Ritchie PA, Thomas DA, Lu LW, Conelly GM. External reinforcement of concrete beams using fiber reinforced plastics. *ACI Struct. J*. 1991;88(4).
8. Triantafillou TC, Plevris N. Strengthening of RC beams with epoxy-bonded fiber composite materials. *Mater. Struct*. 1992;25(4):201–211.
9. Norris T, Saadatmanesh H, Ehsani MR. Shear and flexural strengthening of RC beams with carbon fiber sheets. *J. Struct. Eng*. 1997;123(7):903–911.
10. Akbarzadeh H, Maghsoudi AA. Experimental and analytical investigation of reinforced high strength concrete continuous beams strengthened with fiber reinforced polymer. *Mater. Des*. 2010;31(3):1130–1147.
11. Attari N, Amziane S, Chemrouk M. Flexural strengthening of concrete beams using CFRP, GFRP and hybrid FRP sheets. *Constr. Build. Mater*. 2012;37:746–757.
12. Sharaky IA, Torres L, Baena M, Vilanova I. Effect of different material and construction details on the bond behaviour of NSM FRP bars in concrete. *Constr. Build. Mater*. 2013;38:890–902.
13. Zhou Y, Gou M, Zhang F, Zhang S, Wang D. Reinforced concrete beams strengthened with carbon fiber reinforced polymer by friction hybrid bond technique: Experimental investigation. *Mater. Des*. 2013;50:130–139.
14. Oguz Gunes, Denvid Lau, Chakrapan Tuakta, Oral Büyüköztürk. Ductility of FRP–concrete systems: Investigations at different length scales. *Construction and Building Materials*. 2013;49:915–925.
15. Qeshta IM, Shafigh P, Jumaat MZ, Abdulla AI, Ibrahim Z, Alengaram UJ. These of wire mesh–epoxy composite for enhancing the flexural performance of concrete beams. *Mater. Des*. 2014;60:250–259.
16. Gamal Ismail Khaleel. Strengthening and repair of reinforced concrete beams in flexure using GFRP sheets; 2002.
17. Gamal IK, Debaiky AS, Marwa IA. Ductility of strengthened beams with lap splices. *Engineering Research Journal, Minoufiya University*. 2016;39(4):285-300.
18. Raafat El-Hacha, Sami H. Rizkalla. Near-surface-mounted fiber-reinforced polymer reinforcements for flexural strengthening of concrete structures. *ACI Structural Journal*. 2004;717-727.
19. Jung WT, Park YH, Park JS, Kang JY, You YJ. Experimental investigation on flexural behavior of RC beams strengthened by NSM CFRP reinforcements. *ACI Special Publication*. 2005;230:795-806.
20. Tang WC, Balendran RV, Nadeem A, Leung HY. Flexural strengthening of reinforced lightweight polystyrene aggregate concrete beams with near surface mounted GFRP bars. *Build. Environ*. 2006;41(10):1381–1393.
21. Al-Mahmoud F, Castel A, François R, Tourneur C. Strengthening of RC members with near-surface mounted CFRP rods. *Compos. Struct*. 2009;91(2):138–147.
22. Almusallam TH, Elsanadedy HM, Al-Salloum YA, Alsayed SH. Experimental and numerical investigation for the flexural strengthening of RC beams using near-surface mounted steel or GFRP bars. *J. of*

- Construction and Building Materials. 2013;40:145-161.
23. Sharaky IA, Torres L, Comas J, Barris C. Flexural response of reinforced concrete (RC) beams strengthened with near surface mounted (NSM) fiber reinforced polymer (FRP) bars. Compos. Struct. 2014;109:8–22.
24. Bilotta A, Ceroni F, Nigro E, Pecce M. Efficiency of CFRP NSM strips and EBR plates for flexural strengthening of RC beams and loading pattern influence. Compos. Struct. 2015;124:163-175.
25. El-Gamal SE, Al-Nuaimi A, Al-Saidy A, Al-Lawati A. Efficiency of near surface mounted technique using fiber reinforced polymers for the flexural strengthening of RC beams. Construction and Building Materials. 2016;118:52-62.

© 2019 Makhlouf; This is an Open Access article distributed under the terms of the Creative Commons Attribution License (<http://creativecommons.org/licenses/by/4.0>), which permits unrestricted use, distribution, and reproduction in any medium, provided the original work is properly cited.

Peer-review history:
The peer review history for this paper can be accessed here:
<http://www.sdiarticle3.com/review-history/49847>